JOURNAL OF PROPULSION AND POWER
Vol. 10, No. 5, Sept.–Oct. 1994

Droplet Transport in a Swirl-Stabilized Spray Flame

C. Presser,* A. K. Gupta,† H. G. Semerjian,‡ and C. T. Avedisian§
National Institute of Standards and Technology, Gaithersburg, Maryland 20899

Droplet transport processes that occur in fuel sprays and spray flames were examined using laser velocimetry, phase Doppler interferometry, and laser sheet beam photography. Droplet size and velocity (axial and radial) distributions were obtained in a swirl-stabilized, pressure-atomized kerosene spray under nonburning and burning conditions. The results show that the introduction of swirl to the combustion air (under nonburning conditions) significantly modifies the spray structure and leads to the transport of smaller size droplets from downstream positions of the spray to upstream near the nozzle exit. Time-based velocity data at different spatial locations of the spray indicated some intermittency in the spray and clustering of droplets. In the center of the spray, near the nozzle exit, most of the droplets are recirculated; near the spray boundary, bimodal velocity distributions indicate the presence of recirculated droplets and droplets that arrive directly from the injector. Combustion results in a significant increase in droplet velocities, especially near the spray boundary where the flame sheet resides. The size of the recirculation zone is much reduced with combustion; however, a number of smaller droplets are still transported upstream. The data demonstrate the important role droplet transport plays in providing a fuel vapor feedback mechanism for flame stability.

I. Introduction

FUEL spray atomization is widely used to introduce fuel into the combustion chamber of propulsion and power systems. Pressure-jet swirl atomizers are used extensively for liquid fuel injection in a wide range of aircraft, marine and gas turbine combustors, liquid rocket engines, furnaces, and internal combustion engines. In these atomizers, fuel is introduced into a swirl chamber to provide a high angular component of velocity to enhance the atomization process. The liquid emerging from the nozzle orifice disintegrates into ligaments and finally into droplets to yield a hollow-cone spray. Several recent studies have shown that combustion of fuel sprays is a complicated phenomenon, involving complex physical and chemical processes.[1,2] In turbulent, high-velocity flows, flame stabilization is accomplished by creating flow recirculation, which transports hot combustion products upstream toward the nozzle exit. This feedback mechanism provides reduced ignition times and enhanced combustion rates. Flow recirculation can be established either by using a geometry which provides a sudden expansion to the stream, or by introducing swirl to the combustion air. In addition to recirculation of combustion products, swirl is expected to influence droplet/air mixing and modify the trajectory of droplets in the spray. Its influence is especially apparent near the spray boundary where droplets of many different sizes, traveling at different velocities, are found.

This article examines the structure of a pressure-atomized fuel spray flame, which is stabilized with a swirling combustion airstream. The specific question of interest is the role of droplet transport in the feedback process; viz., are droplets transported upstream near the fuel injector by the recirculating air, or are droplets not entrained by the airstream, and therefore do not contribute to the feedback mechanism? If droplets are recirculated, is the transport process influenced preferentially according to size and velocity? It is generally assumed that only gaseous species (vaporized fuel or combustion products) are transported upstream. To address these issues, a pressure-atomized spray system was examined under nonburning and burning conditions. Results are presented on droplet mean velocity, as well as size and velocity distributions, at various positions in the spray. Laser velocimetry was used to obtain spatially resolved information on the distribution of gas and droplet velocities as a function of radial position. Temporally and spatially resolved information on droplet size and velocity was obtained using phase Doppler interferometry. Laser sheet beam photography was used for direct examination of the spray features.

II. Experimental Apparatus

Experiments were carried out in a spray combustion facility that was designed to simulate practical combustion systems. The facility permits examination of the effects of combustion air swirl, fuel and nozzle type, and air preheat on spray characteristics, under nonburning and burning conditions. The facility includes a swirl burner with a movable 12-vane swirl cascade; the vanes rotate simultaneously to impart the desired degree of swirl to the combustion air that surrounds a pressure-jet nozzle.[3,4] For the nonburning spray experiments, a propane-fueled, ring-shaped afterburner, located at approximately 300 mm downstream of the nozzle, was used to burn the droplets before entering the exhaust canopy. Results in this article are presented for a nominal 60-deg hollow-cone, pressure-atomized kerosene spray, with both coflowing nonswirling ($S = 0$) and swirling ($S = 0.53$) combustion air. The swirl number S refers to the ratio of the axial fluxes of angular momentum to linear momentum.[5] The value of $S = 0.53$ was chosen because it is characteristic of values used in many practical systems (e.g., furnaces),[5] and provided good flame stability while operating the burner. In contrast to a previous study,[6] the effects of primary air were isolated in order to focus on droplet interactions with the surrounding combustion airstream. The total air and fuel flow rates were 64.3 kg/h and 3.2 kg/h, respectively. A stepper-motor-controlled, three-dimensional traversing arrangement was used to translate the burner assembly without disturbing the optics which surround the burner. This permits precise alignment of the optical diagnostic equipment with the spray, and allows spatially resolved measurements of the spray and flame properties to be

Received June 8, 1992; revision received Jan. 5, 1994; accepted for publication Jan. 7, 1994.

*Research Engineer, Chemical Science and Technology Laboratory.
†Professor, Department of Mechanical Engineering, University of Maryland, College Park, MD 20742.
‡Director, Chemical Science and Technology Laboratory.
§Professor, Sibley School of Mechanical and Aerospace Engineering, Cornell University, Ithaca, NY 14853.

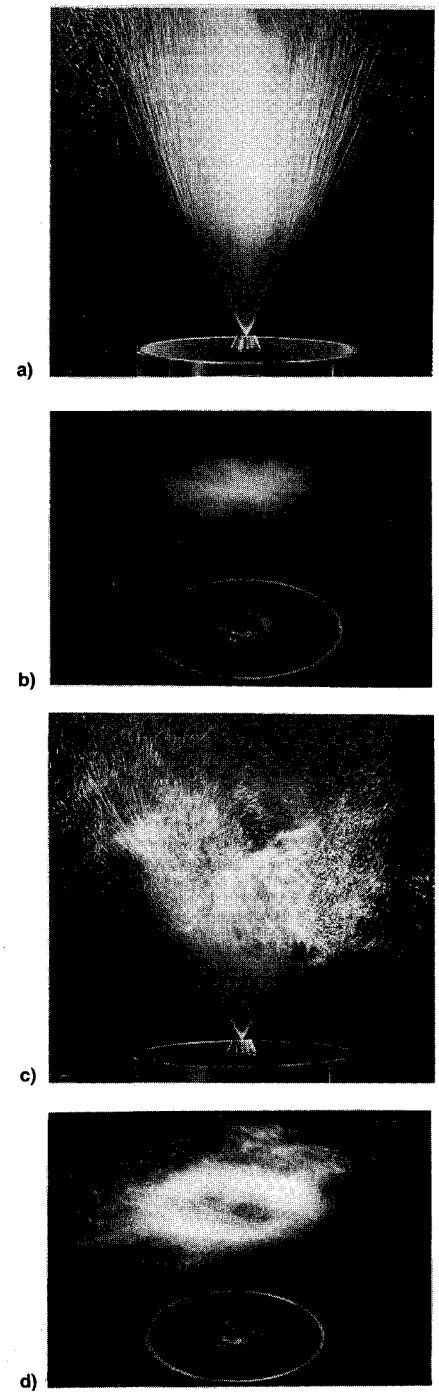

Fig. 1 Kerosene spray structure observed with a laser sheet beam under nonburning conditions at $S = 0$: a) vertical cross section and b) horizontal cross section; and at $S = 0.53$: c) vertical cross section and d) horizontal cross section.

obtained at different positions. Additional details of the experimental facility are given in Ref. 6.

Gas and droplet velocity distributions were obtained initially using a single-channel, dual-beam laser velocimeter (LV). The gas velocity measurements were carried out by seeding the combustion airflow with Al_2O_3 particles (with a nominal size of 1 μm).[6] The measurements were carried out using off-axis light collection optics, positioned at a scattering angle of 30 deg, which provided the necessary spatial resolution. The measurement volume dimensions were 0.316 mm waist (based on the e^{-2} light modulation contour) by 1.08 mm length. The LV system used a 4-W Ar-ion cw laser, operating at a wavelength of 514.5 nm, as the light source and incorporated a Bragg cell frequency shifter to avoid directional ambiguity in the velocity measurements. Velocity distributions were recorded with a counter-type signal processor coupled to a microprocessor-based data acquisition and processing system. A total of 2500 samples were collected at each spatial position to determine the velocity distributions; this provided a measurement repeatability of better than 5%. The measured distributions were then used to obtain statistical data on mean and rms velocity, skewness, and flatness factors.[6] The arrival time of each detected droplet was also recorded in order to provide information on the time-dependent features of the flow. Further details on the optical configuration are given in Ref. 6.

Additional information on droplet size and velocity distributions were obtained using a two-component phase Doppler interferometer (PDI).[7,8] PDI is similar to a conventional dual-beam laser velocimeter, except that four detectors are located in the receiver assembly. Measurement of the temporal frequency of scattered light from the interference fringe pattern is used to determine the particle velocity; measurement of the phase change from the spatial frequency is used to provide information on particle sizes between 1–300 μm with the optical arrangement employed in this investigation. A 4-W Ar-ion cw laser was used as the light source for the measurements. The measurement volume was defined by the 330-μm laser beam waist and field of view of the off-axis collection optics positioned at a scattering angle of 30 deg. The focal lengths of the transmitting and receiving optics were 495 and 500 mm, respectively. The focal length of the collimating lens was 300 mm. The details of the optical arrangement are described in Ref. 9. In principle, the phase Doppler system can be used to measure gas velocity, however, detection of the small-size seed particles would be difficult within the size range of this particular optical configuration. The LV system easily permits such measurements. Comparison of the values of mean velocity for both instruments was in good agreement at the same spatial position and flow conditions. It is recognized that although the dynamic range of the two instruments is somewhat different, they both provide useful information with regard to their sensitivity and selectivity.

The global features of the nonburning kerosene spray were observed by passing a laser sheet beam of about 1 mm thickness through different vertical (through the centerline of the spray) and horizontal cross sections. The scattered light was recorded using a 35-mm camera and a video recording system. High background radiation from the burning kerosene spray allowed recording of only the external features of the kerosene flame. Features of the spray within the flame sheet were obtained using *n*-heptane instead of kerosene. *n*-Heptane produced a hybrid colored flame with the upstream portion having a blue hue followed by a luminous yellow zone. In the upstream region, the spray boundary (illuminated by the laser sheet beam) was observed clearly within the surrounding blue portion of the flame. A variety of filters were also used to attenuate the contribution of the luminous flame region.

III. Results and Discussion

A. Global Spray Features

The global structure of the spray was observed to be influenced significantly by the degree of swirl introduced to the combustion air. This effect was recorded photographically using laser sheet beam illumination to visualize vertical and horizontal cross sections of the spray under nonburning and burning conditions. A representative set of images of a nonburning kerosene spray is shown in Fig. 1 for $S = 0$ and 0.53. The fuel is burned further downstream with the propane-fuelled afterburner. The higher concentration of droplets observed in the center of the spray for $S = 0$ (see Fig. 1a) is attributed to the specific design of the nozzle. The spoke-like pattern for $S = 0$, seen in the horizontal cross section at $z = 76.2$ mm (see Fig. 1b), is due to several small imperfections that form around the orifice lip at the nozzle exit after its initial use. This was verified with an unused nozzle which

produced an uniform distribution of droplets across the spray, without the presence of spokes. (Note that the quantitative data presented in this article were obtained with an initially unused nozzle.) A closer examination of the nozzle orifice revealed a correlation between the number of spokes observed and the number of surface imperfections in the lip.

Combustion air swirl modifies the spray pattern significantly, as shown in Figs. 1c and 1d. At a moderate swirl strength, e.g., $S = 0.53$, the presence of a toroidal recirculation zone displaces droplets found near the centerline towards the outer edge of the spray (see Fig. 1c). This results in a donut-shaped horizontal cross section (see Fig. 1d), with a large number of droplets observed outside the nominal spray boundary. Some of these droplets are transported from downstream locations near the spray boundary to upstream positions near the nozzle. Droplets are then transported radially outward from the spray boundary to be entrained into the surrounding combustion air flowfield. For stronger swirl intensities, droplets can enter the combustion air passage, as observed with a horizontal laser sheet beam positioned at $z = 1$ mm.[6,10] Combustion air swirl therefore strongly influences the global droplet transport process in the spray.

The high background radiation from the kerosene flame prevented examination of the internal spray features with the laser sheet beam. Observation of the spray within the flame sheet was accomplished using *n*-heptane which developed a hybrid color flame, i.e., a nonluminous upstream region followed by a luminous zone. The hollow-cone nature of the spray is preserved within the flame regardless of fuel type; fuel nozzle design generally controls the spray structure (or dispersion of droplets) while fuels of different physical properties affect flame luminosity and the degree of radiative heat transfer.[11] Vertical and horizontal cross-sectional views of the burning *n*-heptane spray are presented in Figs. 2 and 3, respectively, for varying swirl strength. The global features of the spray are similar to the nonburning case, e.g., under swirling conditions the spray cross section is donut-shaped. As swirl strength increases the luminous region of the flame moves upstream toward the burner exit (eventually entering the combustion air passage) and envelops the nonluminous region and spray. Movement of the flame front into the combustion air passage for high swirl strength also occurred for the kerosene flame.[6] The increased swirl strength caused the illuminated spray cone to widen in the upstream region of the flame (compare Figs. 2a–2d), and the increased radiation caused the illuminated thickness of the spray boundary to decrease (compare Figs. 3a–3d).

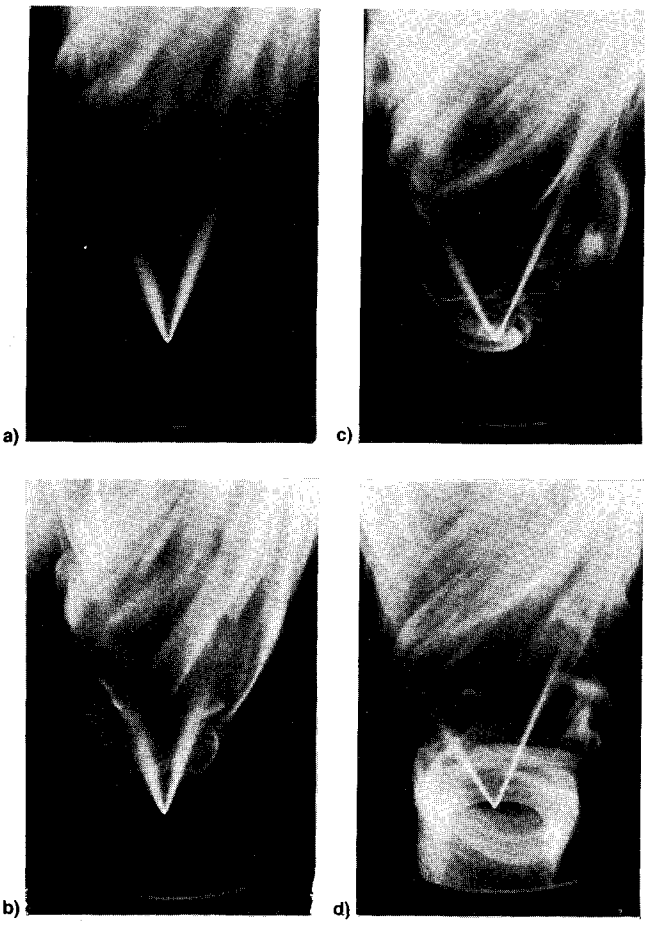

Fig. 2 *n*-Heptane spray structure observed with a vertical laser sheet beam (through the spray centerline) under burning conditions at S = a) 0.39, b) 0.46, c) 0.53, and d) 0.63.

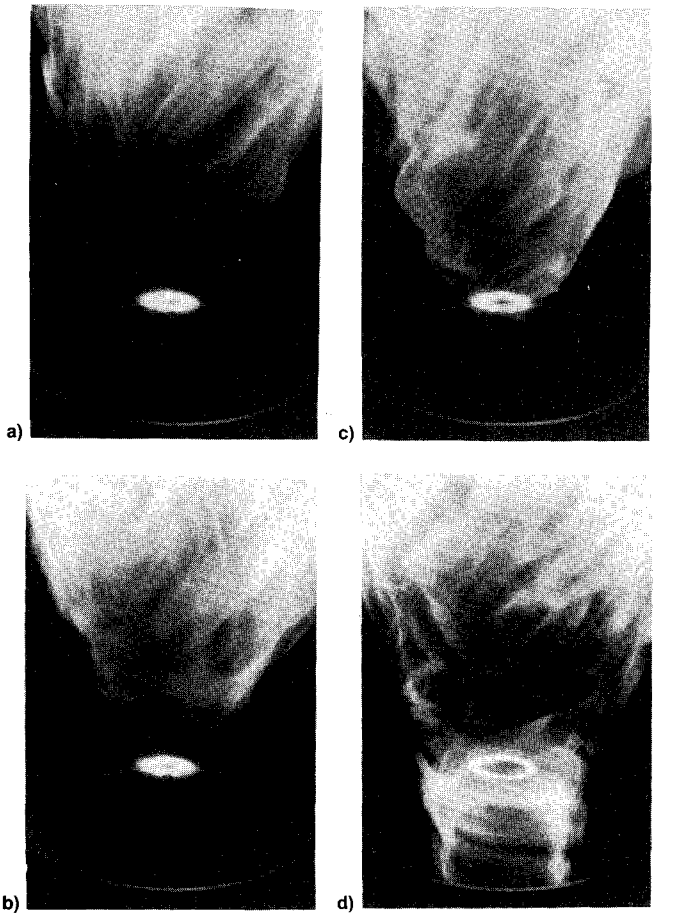

Fig. 3 *n*-Heptane spray structure observed with a horizontal laser sheet beam under burning conditions at $z = 15$ mm for S = a) 0.39, b) 0.46, c) 0.53, and d) 0.63.

B. Droplet Velocity Measurements

To assess quantitatively the effect of combustion air swirl on droplet transport in the kerosene spray, radial profiles of the axial, radial, and tangential components of droplet velocity were obtained at various axial positions downstream of the nozzle exit. The measured tangential velocity profiles (not shown here) indicate that, initially, some tangential velocity is imparted to the fuel droplets by the swirler located inside the nozzle. The tangential air velocity component was also negligible.[6] This velocity component decays rapidly to a value similar to that of the air velocity. Therefore, the emphasis in this article is placed on droplet axial and radial velocities, since they provide direct information on droplet recirculation.

Typical results for the axial U velocity profiles are presented in Fig. 4, under nonburning conditions for $S = 0$ and 0.53 at $z = 10$, 25.4, 50.8, and 76.2 mm. The solid boxes along the abscissa indicate the position of the swirl burner passages, with the fuel nozzle located at the centerline (combustion airflows through the outer coaxial passage). The results in-

dicate a progressive decrease in velocity, and an increase in jet spread with increased axial distance downstream of the nozzle exit. The lower velocity near the spray centerline, as compared to the spray boundary (defined by the radial position that corresponds to the maximum mean axial velocity), indicates the hollow-cone nature of the spray. Measurements of droplet number density by the ensemble scattering/polarization ratio technique[3] also support this finding (viz., droplet concentrations near the spray centerline are much smaller than near the spray boundary). The profiles indicate some asymmetry in the peak values (particularly near the nozzle exit at $z = 10$ mm) and is attributed to imperfections in the surface of the nozzle lip. Further downstream, combustion air swirl enhances mixing and results in symmetrical profiles. The profiles for the radial and tangential velocity components also indicated similar behavior to that of the axial velocity results.

The effect of combustion air swirl on the droplet velocity is shown in Fig. 4. Near the nozzle exit (see $z = 10$ mm), combustion air swirl is found to have negligible influence on the droplet axial velocity near the spray boundary. However, a significant change is observed near the centerline, where the droplet mean velocity is now nearly 0; this is attributed to the presence of a toroidal recirculation zone, introduced by the swirling combustion air. In addition, a significant concentration of droplets is found outside the spray boundary (i.e., measurements are obtained at larger radial distances) due to the centrifugal action of the swirling airflow. Further downstream, at $z \geq 25$ mm, the combustion air swirl interacts more strongly with the spray (effects due to nozzle degradation become negligible), and therefore has a significant influence on droplet transport processes across the entire profile. Indeed, at $z = 25.4$ and 50.8 mm, negative droplet mean velocities are observed along the centerline, indicating the presence of recirculated droplets. For $S = 0.53$, the droplet velocity at $z = 50.4$ and 76.2 mm decreases much more rapidly

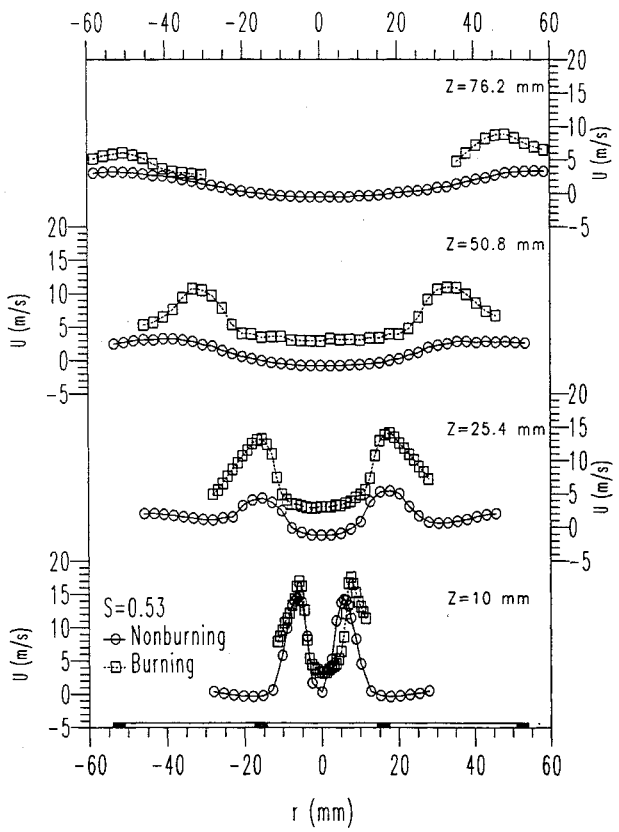

Fig. 4 Radial profiles of droplet mean axial velocity U measured at different axial positions for $S = 0$ and 0.53 under nonburning conditions.

with axial position than for the nonswirling case due to increased droplet/air interaction. Near the spray boundary, the axial velocity for the swirling case decays to a value approximately equal to the surrounding air velocity of about 3 m/s (air velocity profiles are given in Ref. 6). Entrainment of recirculated droplets into the combustion air flowfield therefore is found to enhance fuel/air mixing and fuel vaporization, and provide a fuel vapor feedback mechanism for flame stability.

To provide more detailed information on droplet transport upstream along the spray centerline, droplet size distributions were measured in this region along with the axial U and radial V velocity distributions. Results obtained with the phase Doppler system at axial positions of $z = 10$, 25.4, 50.8, and 76.2 mm under swirling (nonburning) conditions are presented in Fig. 5. The solid bars of the size distribution represent the measured data on a flux (or temporal) basis, while the open bars represent the data corrected for variations in the effective measurement volume.[12] Also note the change in abscissa scale of the diameter and axial velocity distributions for Fig. 5a. The distributions indicate that there is a wide range of droplet sizes and velocities (including positive and negative values) along the spray centerline, although the mean axial velocity is nearly 0. Indeed, the magnitude of the negative droplet velocities increases with decreasing axial position, indicating an accelerating field in the opposite direction to the main flow (cf., Figs. 5a–5d). This is in agreement with the airflow velocity measurements obtained in other investigations,[6,13] which also indicate larger negative velocities near the fuel injector. At $z = 10$ mm (see Fig. 5a) many droplets are detected moving in the downstream direction (positive peak of the bimodal distribution); these droplets are thought to originate directly from the nozzle. The wide range of both positive and negative radial velocities at the various positions indicate that droplets are entrained into the central recirculation vortex before turning downstream. The range of droplet sizes that are entrained by the recirculation zone is indicated by correlating the droplet sizes and velocities. Figure 6 presents the axial velocity/size and radial velocity/size correlations along the spray centerline at the $z = 10$, 25.4, 50.8, and 76.2 mm. The results indicate that there is a wide range of droplet sizes (up to 60 μm) that are associated with the negative axial velocities. There is a greater tendency for the smaller droplets to be associated with a negative axial velocity. At downstream positions (e.g., $z = 76.2$ mm, see Fig. 6d), droplet transport is essentially along the spray centerline. At $z = 10$ mm (see Fig. 6a) the smaller droplets have a wider range of axial and radial velocities than at positions further downstream because of the presence of droplets originating from the nozzle (positive axial and radial values). These results clearly demonstrate that the recirculating flowfield established by the swirling airflow is strong enough to entrain droplets and transport them upstream toward the nozzle exit.

The effect of combustion on the fuel spray is demonstrated in Fig. 7, where velocity profiles for both the burning and nonburning cases are presented for comparison. The results indicate a significant acceleration (or more correctly a lack of deceleration) of droplets at all locations in the flowfield. This is attributed, in part, to the increased volumetric flow rate induced by the combustion process. The reduced strength of the recirculation zone due to combustion (as indicated by the smaller absolute values of negative axial velocity) contributes to the entrainment of fewer droplets. It is also expected that rapid droplet vaporization will reduce the presence of smaller droplets and increase detection of larger droplets with higher axial velocities. This result is confirmed by the size distribution obtained in the flame at $z = 10$ mm (see Fig. 8); in this case, the Sauter mean diameter is 40.0 μm, whereas in the nonburning case it was 18.7 μm (see Fig. 5a). In addition, the results for the *mean* axial droplet velocities (both along the centerline or outside the spray) indicate no negative velocities in the presence of combustion (see Fig. 7). However, the

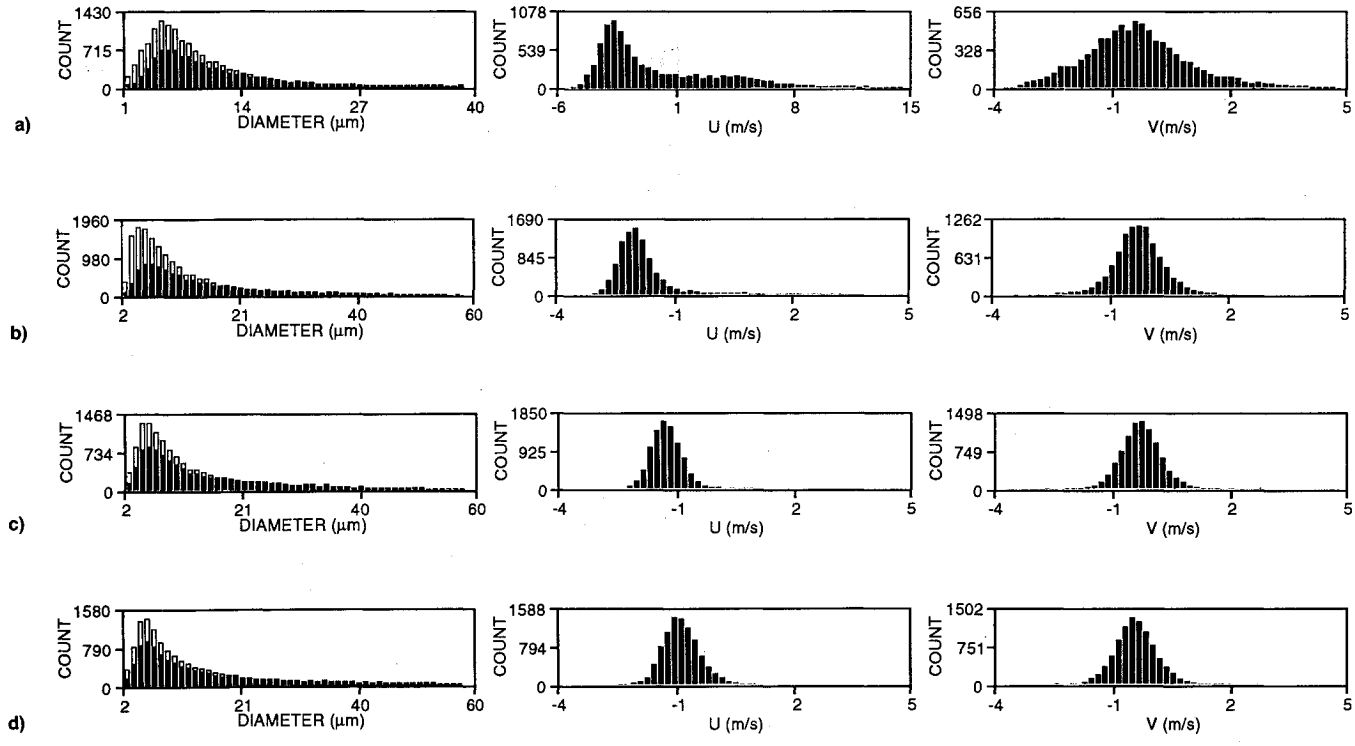

Fig. 5 Droplet size, and axial U and radial V velocity distributions under nonburning conditions along the spray centerline for different axial positions: a) 10, b) 25.4, c) 50.8, and d) 76.2 mm.

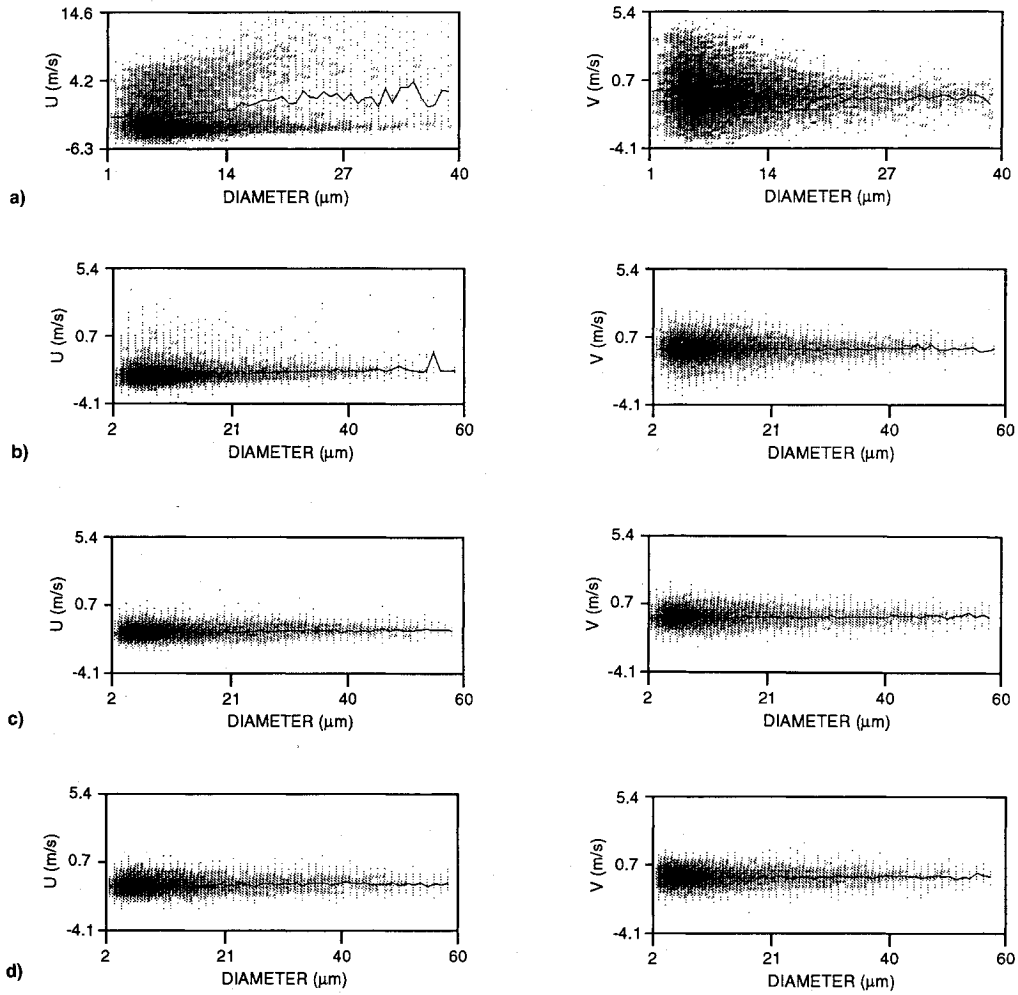

Fig. 6 Axial velocity/diameter and radial velocity/diameter correlations under nonburning conditions along the spray centerline for different axial positions: a) 10, b) 25.4, c) 50.8, and d) 76.2 mm.

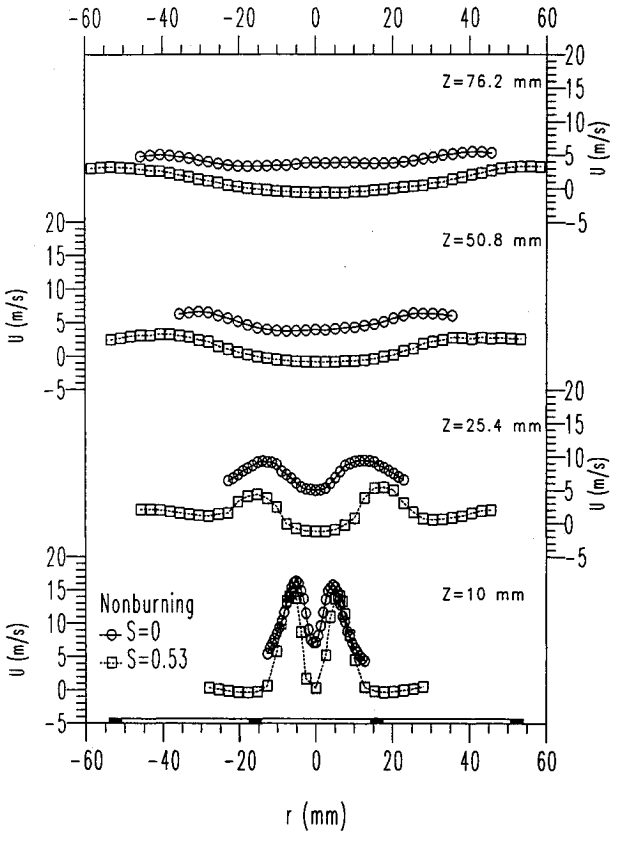

Fig. 7 Radial profiles of droplet mean axial velocity U measured at different axial positions under nonburning and burning conditions for $S = 0.53$.

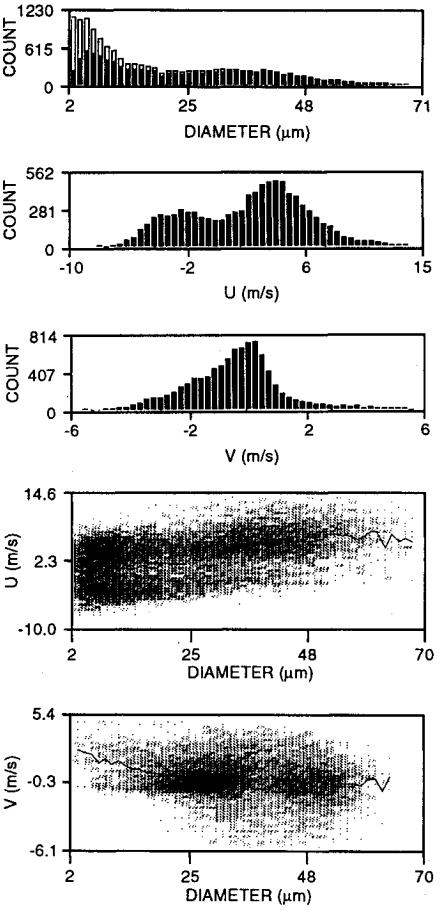

Fig. 8 Droplet size, and axial U and radial V velocity distributions under burning conditions along the spray centerline at $z = 10$ mm.

velocity distributions obtained with the phase Doppler system indicate again that a wide range of droplet sizes and velocities are actually present at this position (see Fig. 8). In fact, the axial velocity distribution indicates the presence of recirculated droplets at this position. The velocity/size correlations for the axial and radial velocity components confirm that smaller size droplets are recirculated, albeit many more droplets (both small and large) are accelerated downstream by the combusting flowfield. Similar observations are also made at z = 25.4 mm. This small vortex persists in spite of the reduced effect of the combustion air swirl. These findings clearly demonstrate the presence of droplets that travel upstream in the combusting flowfield to assist in the feedback of fuel vapor for flame stability.

C. Time-Based Droplet Velocity Measurements

The simultaneous presence of droplets with negative and positive velocities in many parts of the spray and spray flame leads to questions about the possible intermittent nature of the flowfield. The question of interest is whether droplets traveling in opposite directions arrive at a spatial position at random and in a continuous manner, or do droplets arrive intermittently with discrete occurrence of frequencies. To address this issue, data were obtained on the time-of-arrival of all droplets that were detected at each position with the laser velocimeter. Data obtained for z = 10 mm at the centerline and spray boundary, under nonburning and burning conditions, are presented in Fig. 9. For the spray boundary results, data are presented at positions where the mean droplet velocity is maximum. As a result, data being compared were obtained at slightly different radial positions; flow acceleration due to combustion near the flame front moved the location of the maximum axial velocity radially outward.

At the center of the spray, in the nonburning case (see Fig. 9a), droplets traveling upstream (i.e., those with negative velocities) constitute the majority of the droplets. In contrast, droplets with larger positive velocities pass intermittently (i.e., with less frequency) through the measurement volume; these are the droplets that arrive directly from the fuel injector, and are traveling in the direction opposite to the recirculated droplets. In the burning case (see Fig. 9b), fewer droplets are found with negative axial velocity (compare Figs. 9a and 9b). The data in Figs. 9a and 9b indicate that droplet transport is not completely random, but contain considerable clustering of droplets (i.e., groups of droplets with similar values of axial velocity which enter the measurement volume with relatively small interarrival times). Quantitative analysis of the randomness and intermittency of droplet transport in spray flames is currently under investigation.[9,14]

Near the spray boundary, in the nonburning case (see Fig. 9c), most of the droplets are traveling at a considerably higher velocity than at $r = 0$ without much interaction with the airflow; arrival times of these droplets are quite random. There are, however, smaller droplets with much lower velocities that arrive less frequently; these are the recirculated droplets that have been entrained in the airflow. In the burning case (see Fig. 9d), the number of the low velocity droplets is reduced significantly, due to vaporization and combustion, and the high-velocity droplets originating from the injector continue to arrive randomly. The mean axial velocity increased from 14.2 to 17.5 m/s as a result of combustion and the increased volumetric flow rate. Note that the validated data rate is also much higher near the spray boundary than at the spray centerline, with the highest rate obtained for the burning case (compare the number of droplets detected over the same time interval). Higher droplet rejection rates (attributed to the higher droplet number densities) for the nonburning case near the spray boundary caused the validated data rate for the burning case to exceed that of the nonburning case (see Figs. 9c and 9d). Based on the above-mentioned results, it can be concluded that some intermittent processes are observed in these sprays and flames. There is some evidence of droplet

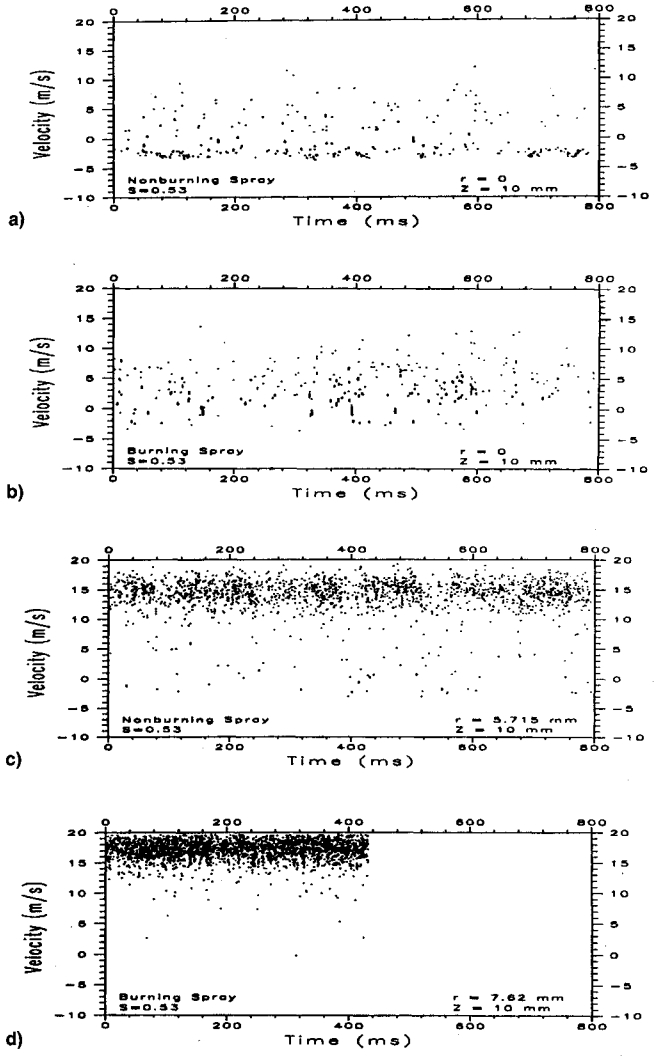

Fig. 9 Time-based droplet axial velocities U obtained with $S = 0.53$ at $z = 10$ mm and at $r =$ a) 0 mm, nonburning spray, b) 0 mm, burning spray, c) 5.7 mm, nonburning spray, and d) 7.6 mm, burning spray.

clustering. The recirculating droplets are observed on a random basis; the intermittent nature of the flow appears to be due to the intermittency of the droplet injection process.

IV. Summary

Size and velocity measurements were carried out in a pressure-atomized kerosene spray under both nonburning and burning conditions. Data were obtained under nonburning conditions both without and with introduction of swirl to the combustion airflow surrounding the spray. Laser velocimetry, phase Doppler interferometry, and laser sheet beam photography were used to examine the droplet transport processes in the fuel spray and spray flames. Swirl was found to have a significant effect on droplet transport in both nonburning and burning spray flames. The introduction of swirl to the combustion airflow creates a central toroidal recirculation zone which promotes the transport of droplets from downstream locations of the spray to upstream location closer to the nozzle exit. In this zone the relatively smaller size droplets are found to be recirculated. These recirculated droplets are then radially dispersed into the surrounding combustion airflow. Time-based velocity measurements obtained with the laser velocimeter showed the random nature of the droplet arrival rate into the measurement volume at all positions in the spray. Near the spray centerline most of the droplets were found to have negative axial velocity associated with the recirculation zone; occasionally, few droplets were found to be traveling with a positive axial velocity. These droplets with positive axial velocity are believed to have arrived directly from the nozzle exit. Near the spray boundary, most of the droplets arrive directly from the nozzle exit (having high positive axial velocity) with detection of few recirculated droplets (having low or negative axial velocity). The simultaneous presence of positively and negatively moving droplets within the small measurement volume may have some implications with regard to the droplet coalescence and dispersion. There is also some evidence of droplet clustering.

In the spray flame, the droplet mean velocities are much higher than those found in the nonburning spray. Combustion also reduces the size and strength of the central recirculation zone. As a result, the droplet mean axial velocity in the center of the spray becomes positive; however, many droplets are still found that travel upstream towards the spray nozzle. The number of these recirculated droplets is much smaller than that found under nonburning conditions. The results presented demonstrate the strong interaction between the spray droplets and the aerodynamic pattern of the combustion air flowfield. They also clearly demonstrate that droplets are entrained by the recirculating air and travel upstream towards the fuel injector. Many of the recirculated droplets vaporize and provide additional fuel vapor for flame stability. Vaporization of these droplets (as opposed to their emission into the environment) also contributes to enhanced combustion efficiency.

Acknowledgments

The authors wish to acknowledge the support of this work by the U.S. Department of Energy, Conservation, and Renewable Energy, Office of Industrial Processes, Advanced Industrial Concepts Division. Neil Rossmeissl and Marvin Gunn are the project monitors. The contributions of one of the authors (C.T.A.) were supported by the New York State Center for Hazardous Waste Management (Ralph R. Rumer, Director). Much appreciation is also due to M. Helfer for the spray and flame photographs, M. J. Carrier for development of the data acquisition and analysis software for the laser velocimetry system, and J. D. Allen for technical support.

References

[1]Faeth, G. M., "Evaporation and Combustion of Sprays," *Progress in Energy and Combustion Science*, Vol. 9, Nos. 1/2, 1983, pp. 1–76.

[2]Sirignano, W. A., "Fuel Droplet Vaporization and Spray Combustion Theory," *Progress in Energy and Combustion Science*, Vol. 9, No. 4, 1983, pp. 291–322.

[3]Presser, C., Gupta, A. K., Semerjian, H. G., and Santoro, R. J., "Droplet/Air Interaction in a Swirl-Stabilized Spray Flame," *Proceedings of the ASME/JSME Thermal Engineering Joint Conference* (Honolulu, HI), 1987, pp. 73–83.

[4]Presser, C., Gupta, A. K., Santoro, R. J., and Semerjian, H. G., "Velocity and Droplet Size Measurements in a Fuel Spray," AIAA Paper 86-0297, Jan. 1986.

[5]Gupta, A. K., Lilley, D. G., and Syred, N., *Swirl Flows*, Abacus Press, Kent, England, UK, 1984.

[6]Presser, C., Gupta, A. K., and Semerjian, H. G., "Aerodynamic Characteristics of Swirling Spray Flames: Pressure-Jet Atomizer," *Combustion and Flame*, Vol. 92, Nos. 1/2, 1993, pp. 25–44.

[7]Bachalo, W. D., Houser, M. J., and Smith, J. N., "Evolutionary Behavior of Sprays Produced by Pressure Atomizers," AIAA Paper 86-0296, Jan. 1986.

[8]Bachalo, W. D., and Houser, M. J., "Phase/Doppler Spray Analyzer for Simultaneous Measurements of Drop Size and Velocity Distributions," *Optical Engineering*, Vol. 23, No. 5, 1984, pp. 583–590.

[9]Presser, C., and Gupta, A. K., "Behavior of Droplets in Pressure-Atomized Fuel Sprays with Coflowing Air Swirl," *Heat Transfer in Fire and Combustion Systems*, edited by B. Farouk, M. P. Menguc, R. Viskanta, C. Presser, and S. Chellaiah, HTD-Vol. 250, American Society of Mechanical Engineers, New York, 1993, pp. 79–92.

[10]Presser, C., Gupta, A. K., and Semerjian, H. G., "Dynamics of

Pressure-Jet and Air-Assist Nozzle Sprays: Aerodynamic Effects," AIAA Paper 88-3139, July 1988.

[11]Presser, C., Gupta, A. K., Avedisian, C. T., and Semerjian, H. G., "Fuel Property Effects on the Structure of Spray Flames," *Twenty-Third Symposium (International) on Combustion*, The Combustion Inst., Pittsburgh, PA, 1991, pp. 1361–1367.

[12]Bachalo, W. D., Houser, N. J., and Smith, J. N., "Behavior of Sprays Produced by Pressure Atomizers as Measured Using a Phase/Doppler Instrument," *Atomization and Spray Technology*, Vol. 3, No. 1, 1987, pp. 53–72.

[13]Edwards, C. F., and Rudoff, R. C., "Structure of a Swirl-Stabilized Spray Flame by Imaging, Laser Doppler Velocimetry, and Phase Doppler Anemometry," *Twenty-Third Symposium (International) on Combustion*, The Combustion Inst., Pittsburgh, PA, 1991, pp. 1353–1359.

[14]Zurlo, J. R., Presser, C., and Gupta, A. K., "Time-Based Analysis of Phase/Doppler Data," *Laser Applications in Combustion and Combustion Diagnostics*, edited by L. C. Liou, Vol. 1862, SPIE-The Int'l Society for Optical Engineering, Bellingham, WA, 1993, pp. 141–153.